

# Applications of Nanomaterials

## 9.1. Introduction

Nanotechnology offers an extremely broad range of potential applications from electronics, optical communications and biological systems to new materials. Many possible applications have been explored and many devices and systems have been studied. More potential applications and new devices are being proposed in literature. It is obviously impossible to summarize all the devices and applications that have been studied and it is impossible to predict new applications and devices. This chapter will simply provide some examples to illustrate the possibilities of nanostructures and nanomaterials in device fabrication and applications. It is interesting to note that the applications of nanotechnology in different fields have distinctly different demands, and thus face very different challenges, which require different approaches. For example, for applications in medicine, or in nanomedicine, the major challenge is "miniaturization": new instruments to analyze tissues literally down to the molecular level, sensors smaller than a cell allowing to look at ongoing functions, and small machines that literally circulate within a human body pursuing pathogens and neutralizing chemical toxins.<sup>1</sup>

Applications of nanostructures and nanomaterials are based on (i) the peculiar physical properties of nanosized materials, e.g. gold

nanoparticles used as inorganic dye to introduce colors into glass and as low temperature catalyst, (ii) the huge surface area, such as mesoporous titania for photoelectrochemical cells, and nanoparticles for various sensors, and (iii) the small size that offers extra possibilities for manipulation and room for accommodating multiple functionalities.) For many applications, new materials and new properties are introduced. For example, various organic molecules are incorporated into electronic devices, such as sensors.<sup>2</sup> This chapter intends to provide some examples that have been explored to illustrate the vast range of applications of nanostructures and nanomaterials.

## 9.2. Molecular Electronics and Nanoelectronics

Tremendous efforts and progress have been made in the molecular electronics and nanoelectronics.<sup>3-12</sup> In molecular electronics, single molecules are expected to be able to control electron transport, which offers the promise of exploring the vast variety of molecular functions for electronic devices, and molecules can now be crafted into a working circuit as shown schematically in Fig. 9.1.<sup>3</sup> (When the molecules are biologically active, bioelectronic devices could be developed.<sup>2,13</sup> In molecular electronics, control over the electronic energy levels at the surface of conventional semiconductors and metals is achieved by assembling on the solid

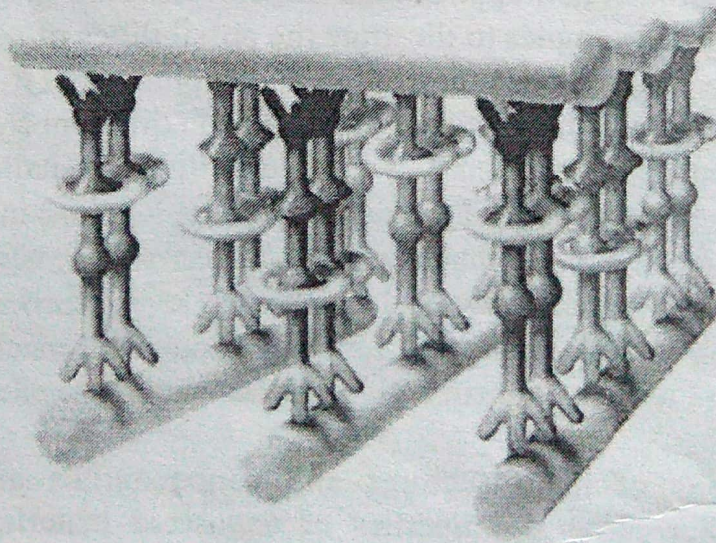


Fig. 9.1. Schematic showing that molecules can now be crafted into working circuit, though constructing real molecular chips remains a big challenge. [R. F. Service, *Science* 293, 782 (2001).] <http://hhud.tvu.edu.vn>

surfaces, poorly organized, partial monolayers of molecules instead of the more commonly used ideal ones. Once those surfaces become interfaces, these layers exert electrostatic rather than electrodynamic control over the resulting devices, based on both electrical monopole and dipole effects of the molecules. Thus electronic transport devices, incorporating organic molecules, can be constructed without current flow through the molecules. The simplest molecular electronics are sensors that translate unique molecular properties into electrical signals. Sensors using a field effect transistor (FET) configuration with its gate displaced into a liquid electrolyte, and an active layer of molecules for molecular recognition were reported in early 1970's.<sup>14</sup> A selective membrane is inserted on the insulator surface of the FET, and this permits the diffusion of specific analyte ions and construction of a surface dipole layer at the insulator surface. Such a surface dipole changes the electric potential at the insulator surface and, thus, permits the current going through the device. Such devices are also known as ion-selective FET (ISFET) or chemical FET (CHEM-FET).<sup>2,15,16</sup> Thin films attached to metal nanoparticles have been shown to change their electrical conductivity rapidly and reproducibly in the presence of organic vapors, and this has been exploited for the development of novel gas sensors.<sup>17,18</sup> The monolayer on metal nanoparticles can reversibly adsorb and desorb the organic vapor, resulting in swelling and shrinking of the thickness of the monolayer, thus changing the distance between the metal cores. Since the electron hopping conductivity through the monolayers is sensitively dependent on the distance, the adsorption of organic vapor increases the distance and leads to a sharp decrease in electrical conductivity.

Many nanoscale electronic devices have been demonstrated: tunneling junctions,<sup>19-21</sup> devices with negative differential resistance,<sup>22</sup> electrically configurable switches,<sup>23,24</sup> carbon nanotube transistors,<sup>25,26</sup> and single molecular transistors.<sup>27,28</sup> Devices have also been connected together to form circuits capable of performing single functions such as basic memory<sup>23,24,29</sup> and logic functions.<sup>30-33</sup> Ultrahigh density nanowires lattices and circuits with metal and semiconductor nanowires have also been demonstrated.<sup>34</sup> Computer architecture based on nanoelectronics (also known as nanocomputers) has also been studied,<sup>35,36</sup> though very limited. Various processing techniques have been applied in the fabrication of nanoelectronics such as focused ion beam (FIB),<sup>37-39</sup> electron beam lithography,<sup>34,40</sup> and imprint lithography.<sup>38</sup> Major obstacles preventing the development of such devices include addressing nanometer-sized objects such as nanoparticles and molecules, molecular vibrations, robustness and the poor electrical conductivity.

Au nanoparticles have been widely used in nanoelectronics and molecular electronics using its surface chemistry and uniform size. For example, Au nanoparticles function as carrier vehicles to accommodate multiple functionalities through attaching various functional organic molecules or bio-components.<sup>41</sup> Au nanoparticles can also function as mediators to connect different functionalities together in the construction of nanoscale electronics for the applications of sensors and detectors. Various electronic devices based on Au nanoparticles and Au<sub>55</sub> clusters have been explored.<sup>42-44</sup> In particular, single electron transistor action has been demonstrated for systems that contain ideally only one nanoparticle in the gap between two electrodes separated by only a few nanometers. This central metal particle represents a Coulomb blockade and exhibits single electron charging effects due to its extremely small capacitance. It can also act as a gate if it is independently addressable by a third terminal. An electrochemically addressable nanoswitch, consisting of a single gold particle covered with a small number of dithiol molecules containing a redox-active viologen moiety has been demonstrated, and the electron transfer between the gold substrate and the gold nanoparticle depend strongly on the redox-state of the viologen.<sup>45</sup>

Single-walled carbon nanotubes have also been intensively studied for nanoelectronic devices, due to the semiconducting behavior of different allotropes.<sup>46</sup> Examples of single-walled carbon nanotube nanoelectronic devices include single-electron transistors,<sup>47-49</sup> FET,<sup>30,50,51</sup> sensors,<sup>52,53</sup> circuits,<sup>54</sup> and a molecular electronics toolbox.<sup>55</sup> Carbon nanotubes have been explored for many other applications, such as actuators,<sup>56,57</sup> sensors,<sup>58,59</sup> and thermometers made of multiple-walled carbon nanotubes filled with gallium.<sup>60</sup>

### 9.3. Nanobots

A very promising and fast growing field for the applications of nanotechnology is in the practice of medicine, which, in general, is often referred to as nanomedicine. One of the attractive applications in nanomedicine has been the creation of nanoscale devices for improved therapy and diagnostics. Such nanoscale devices are known as nanorobots or more simply as nanobots.<sup>61</sup> These nanobots have the potential to serve as vehicles for delivery of therapeutic agents, detectors or guardians against early disease and perhaps repair of metabolic or genetic defects. Similar to the conventional or macroscopic robots, nanobots would be programmed to perform specific functions and be remotely controlled, but possess a much smaller size, so that they can travel and perform desired functions inside

the human body. Such devices were first described by Drexler in his book, *Engines of Creation* in 1986.<sup>62</sup>

Haberzettl<sup>61</sup> described what nanobots would do in practice in medicine, which is briefly summarized below. Nanobots applied to medicine would be able to seek out a target within the body such as a cancer cell or an invading virus, and perform some function to fix the target. The fix delivered by the nanobots may be that of releasing a drug in a localized area, thus minimizing the potential side effects of generalized drug therapy, or it may bind to a target and prevent it from further activity thus, for example, preventing a virus from infecting a cell. Further in the future, gene replacement, tissue regeneration or nanosurgery are all possibilities as the technology becomes more mature and sophisticated.

Although such capable and sophisticated nanobots are not yet realized, many functions in much simplified nanobots are being investigated and tested in the lab. It is also being argued that the nanobots would not take the conventional approach of macroscopic robots. Examples include:

- (1) Architecture or structure to carry the payload, known as carrier: Three groups of nanoscale materials have been studied extensively as a structure or vehicle to carry various payloads. The first group is carbon nanotubes or buckyballs, the second group various dendrimers, and the third various nanoparticles and nanocrystals.
- (2) Targeting mechanisms to guide the nanobots to the desired site of action: The most likely mechanisms to be employed are based on antigen or antibody interactions or binding of target molecules to membrane-bound receptors. The navigation system for nanobots would be most likely to use the same method that the human body uses, going with the flow and "dropping anchor" when the nanobots reached its target.
- (3) Communication and information processing: Single molecular electronics may offer simple switch function of on and off, optical labeling would be a more readily achievable reality.
- (4) Retrieve of nanobots from human body: Retrieve of nanobots from human body would be another challenge in the development of nanobots. Most nanodevices could be eliminated from the body through natural mechanisms of metabolism and excretion. Nanodevices made of biodegradable or naturally occurring substances, such as calcium phosphate, would be another favorable approach. "Homing" nanobots would be ideal, which can be collected and removed after performing the desire function. The possible negative impacts of nanobots include the pollution and clog of systems in human body, and the nanobots may become "out of control" when some functions are lost or nanobots malfunction.

## 9.4. Biological Applications of Nanoparticles

Biological applications of colloidal nanocrystals have been summarized in an excellent review article, and the following text is mainly based on this article.<sup>63</sup> One important branch of nanotechnology is nanobiotechnology. Nanobiotechnology includes (i) the use of nanostructures as highly sophisticated scopes, machines or materials in biology and/or medicine, and (ii) the use of biological molecules to assemble nanoscale structures.<sup>63</sup> The following will briefly describe one of the important biological applications of colloidal nanocrystals: molecular recognition. But there are many more biological applications of nanotechnology.<sup>64-66</sup>

Molecular recognition is one of the most fascinating capabilities of many biological molecules.<sup>67,68</sup> Some biological molecules can recognize and bind to other molecules with extremely high selectivity and specificity. For molecular recognition applications, antibodies and oligonucleotides are widely used as receptors. Antibodies are protein molecules created by the immune systems of higher organisms that can recognize a virus as a hostile intruder or antigen, and bind to it in such a way that the virus can be destroyed by other parts of the immune system.<sup>67</sup> Oligonucleotides, known as single stranded deoxyribonucleic acid (DNA), are linear chains of nucleotides, each of which is composed of a sugar backbone and a base. There are four different bases: adenine (A), cytosine (C), guanine (G), and thymine (T).<sup>67</sup> The molecular recognition ability of oligonucleotides arises from two characteristics. One is that each oligonucleotide is characterized by the sequence of its bases, and another is that base A only binds to T and C only to G. That makes the binding of oligonucleotides highly selective and specific.

Antibodies and oligonucleotides are typically attached to the surface of nanocrystals via (i) thiol-gold bonds to gold nanoparticles,<sup>69,70</sup> (ii) covalent linkage to silanized nanocrystals with bifunctional crosslinker molecules,<sup>71-73</sup> and (iii) a biotin-avidin linkage, where avidin is adsorbed on the particle surface.<sup>74,75</sup> When a nanocrystal is attached or conjugated to a receptor molecules, it is "tagged". Nanocrystals conjugated with a receptor can now be "directed" to bind to positions where ligand molecules are present, which "fit" the molecular recognition of the receptor<sup>76</sup> as schematically shown in Fig. 9.2. This facilitates a set of applications including molecular labeling.<sup>63,77-79</sup> For example, when gold nanoparticles aggregate, a change of color from ruby-red to blue is observed, and this phenomenon has been exploited for the development of very sensitive colorimetric methods of DNA analysis.<sup>80</sup> Such devices are capable of detecting trace amounts of a particular oligonucleotide sequence and distinguishing between perfectly

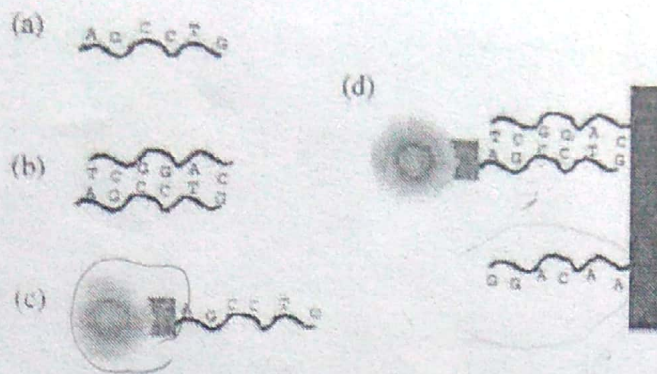


**Fig. 9.2.** DNA as a molecular template to arrange nanoscale objects. (a) One oligonucleotide composed of six bases (A,G,C,C,T,G). (b) One oligonucleotide (AGCCTG) bound to a complementary oligonucleotide. (c) Conjugate formed between a silanized CdSe/ZnS nanocrystal and an oligonucleotide with six bases. (d) The nanocrystal-oligonucleotide conjugate binds to an oligonucleotide with complementary sequence that is immobilized on a surface, but does not bind to oligonucleotides with different sequences. [W.J. Parak, D. Gerion, T. Pellegrino, D. Zanchet, C. Micheel, S.C. Williams, R. Boudreau, M.A. Le Gros, C.A. Larabell, and A.P. Alivisatos, *Nanotechnology* 14, R15 (2003).]

complementary DNA sequences and those that exhibit different degrees of base pair mismatches.

## 9.5. Catalysis by Gold Nanoparticles

Bulk gold is chemically inert and thus considered to be not active or useful as a catalyst.<sup>81,82</sup> However, gold nanoparticles can have excellent catalytic properties as first demonstrated by Haruta.<sup>83</sup> For example, gold nanoparticles with clean surface have demonstrated to be extremely active in the oxidation of carbon monoxide if deposited on partly reactive oxides, such as Fe<sub>2</sub>O<sub>3</sub>, NiO and MnO<sub>2</sub>.  $\gamma$ -alumina,<sup>84</sup> and titania<sup>85,86</sup> are also found to be reactive. Figure 9.3 shows a STM image of Au nanoparticles TiO<sub>2</sub>(110)-(1 × 1) substrate as prepared before a CO:O<sub>2</sub> reaction.<sup>85</sup> The Au coverage is 0.25 ML, and the sample was annealed at 850 K for 2 min. The size of the images is 50 nm by 50 nm.<sup>85</sup> Au nanoparticles also exhibit extraordinary high activity for partial oxidation of hydrocarbons, hydrogenation of unsaturated hydrocarbons and reduction of nitrogen oxides.<sup>83</sup>

The excellent catalytic property of gold nanoparticles is a combination of size effect and the unusual properties of individual gold atom. The unusual properties of gold atom are attributable to the so-called relativistic effect that stabilizes the 6s<sup>2</sup> electron pairs.<sup>81,87</sup> The relativistic effect is briefly described below. As the atomic number increases, so does the mass of nucleus. The speed of the innermost 1s<sup>2</sup> electrons has to increase to maintain their position, and for gold, they attain a speed of 60% light

<http://hhud.tvu.edu.vn>

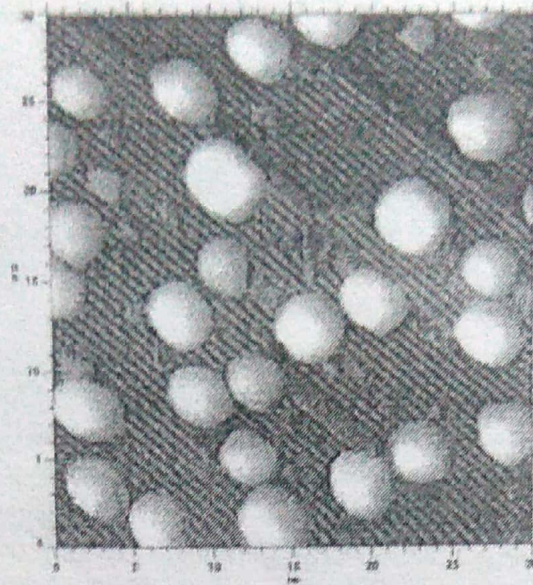


**Fig. 9.3.** A STM image of Au on  $\text{TiO}_2(110)-(1 \times 1)$  substrate as prepared before a  $\text{CO}:\text{O}_2$  reaction. The Au coverage is 0.25 ML, and the sample was annealed at 850 K for 2 min. The size of the images is 30 nm by 30 nm. [Courtesy of Prof. D. Wayne Goodman at Texas A&M University, detailed information seen M. Valden, X. Lai, and D.W. Goodman, *Science* **281**, 1647 (1998).]

speed. A relativistic effect on their mass results in the  $1s$  orbital contraction. Then all the outer  $s$  orbitals have to contract in sympathy, but  $p$  and  $d$  electrons are much less affected. In consequence, the  $6s^2$  electron pair is contracted and stabilized, and the actual size of Au is  $\sim 15\%$  smaller than it would be in the absence of the relativistic effect. Further, much of the chemistry of gold, including the catalytic properties, is therefore determined by the high energy and reactivity of the  $5d$  electrons. This relativistic effect explains why gold differs so much from its neighbors. Essential requirements for high oxidation activity of gold particles include: small particle size (not larger than 4 nm),<sup>88</sup> use of "reactive" support, and a preparative method that achieves the desired size of particle in intimate contact with the support. As the size of gold nanoparticles is sufficiently small, (i) the fraction of surface atoms increases, (ii) the band structure is weak, so surface atoms on such small particles behave more like individual atoms, and a greater fraction of atoms are in contact with the support, and the length of the periphery per unit mass of metals rises.

Thiol-stabilized gold nanoparticles have also been exploited for catalysis applications. Examples include asymmetric dihydroxylation reactions,<sup>89</sup> carboxylic ester cleavage,<sup>90</sup> electrocatalytic reductions by anthraquinone functionalized gold particles<sup>91</sup> and particle-bound ring opening metathesis polymerization.<sup>92</sup> It should be noted that the above-mentioned catalytic applications are based on the carefully designed



chemical functionality of the ligand shell, instead of the potential catalytic activity of a nanostructured clean metal surface.

## 9.6. Band Gap Engineered Quantum Devices

Band gap engineering is a general term referring to the synthetic tailoring of band gaps<sup>93,94</sup> with the intent to create unusual electronic transport and optical effects, and novel devices. Obviously, most of the devices based on semiconductor nanostructures are band gap engineered quantum devices. However, the examples discussed in this section are focused mainly on the device design and fabrication of quantum well and quantum dot lasers by vapor deposition and lithography techniques.

### 9.6.1. Quantum well devices

Lasers fabricated using single or multiple quantum wells based on III-V semiconductors as the active region have been extensively studied over the last two decades. Quantum well lasers offer improved performance with lower threshold current and lower spectra width as compared to that of regular double heterostructure lasers. Quantum wells allow the possibility of independently varying barriers and cladding layer compositions and widths, and thus separate determination of optical confinement and

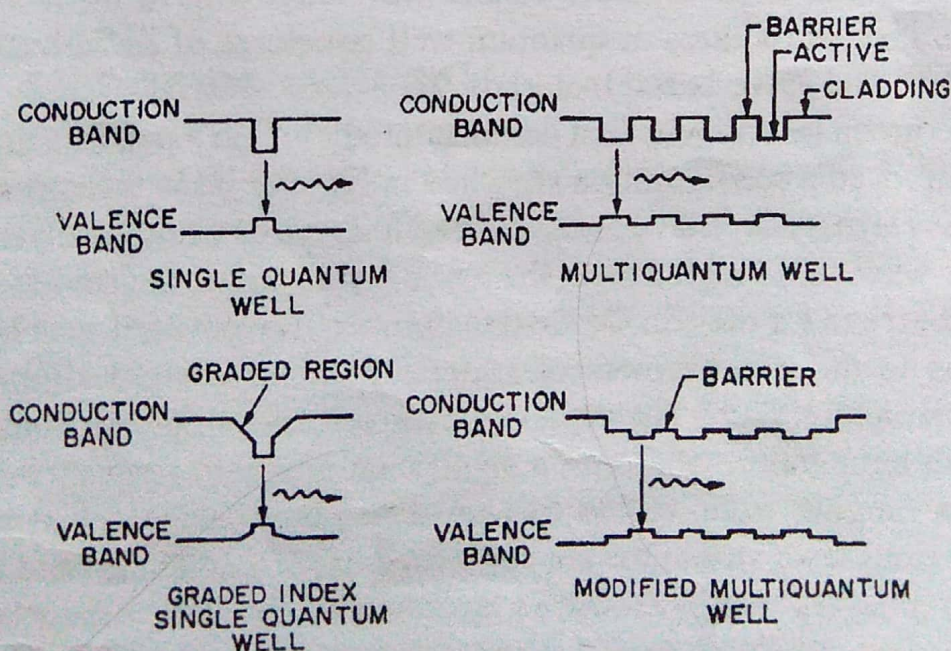


**Fig. 9.4.** Schematic energy band diagrams of different types of quantum well structures used to optimize the laser performance. [P.K. Bhattacharya and N.K. Dutta, *Ann. Rev. Mater. Sci.* 23, 79 (1993).] <http://hhud.tvu.edu.vn>

electrical injection. Quantum well lasers were first fabricated using the GaAs/AlGaAs material systems,<sup>95,96</sup> and Fig. 9.4 shows schematic energy band diagrams of different types of quantum well structures used to optimize the laser performance.<sup>97</sup> One of the main differences between the single quantum well and the multiple quantum well lasers is that the confinement factor of the optical mode is significantly smaller for the former. This results in higher threshold carrier and current densities for single quantum well lasers; however the confinement factor of single quantum well lasers can be significantly increased using a graded-index cladding structure.<sup>98</sup> InGaAsP/InP is another material system used in the fabrication of quantum well lasers.<sup>99,100</sup> InGaAsN/GaAs quantum wells are yet another example.<sup>101</sup> Strain has been explored and introduced into quantum well lasers, since strain can alter the band structure parameters significantly to produce many desirable features such as better high temperature performance resulting from reduced Auger recombination, small chirp, and high bandwidth.<sup>97</sup> Other quantum well optical devices have also been extensively studied and include quantum well electroabsorption and electro-optic modulators, quantum well infrared photodetectors, avalanche photodiodes and optical switching and logic devices.

Blue/green light-emitting diodes (LED) have been developed based on nanostructures of wide-band gap II–VI semiconductor materials.<sup>102</sup> Such devices take direct advantages of quantum well heterostructure configurations and direct energy band gap to achieve high internal radiative efficiency. Various LED at short visible wavelengths have been fabricated based on nanostructures or quantum well structures of ZnSe-based materials<sup>103,104</sup> and ZnTe-based materials.<sup>105</sup>

Blue/green lasers were first demonstrated<sup>106,107</sup> in a p–n injection diode that employed a configuration sketched in Fig. 9.5.<sup>102</sup> In this structure, the Zn(S,Se) ternary layers were introduced to serve as cladding layers for the optical waveguide region with the ZnSe layers and thus provide the electronic barriers for the (Zn,Cd)Se quantum wells. A lot of effects have been devoted to the improvement of materials and structure-design from the above structure.<sup>108,109</sup> The typical blue/green lasers operate continuously at room temperature and emit a significant amount of power with wavelengths ranging from 463 to 514 nm depending on the actual structure. The various laser structures are composed of (Zn,Mg)(Se,S) and Zn(Se,S) cladding layers with (Zn,Cd)Se quantum wells and possess a graded ohmic contact consisting of Au metal on a pseudo-alloy of Zn(Se,Te).

Heterojunction bipolar transistor (HBT) is an example of nanostructured devices based on GeSi/Si nanostructures.<sup>110,111</sup> For this structure, the GeSi layer is thick enough so that no quantum confinement occurs. In

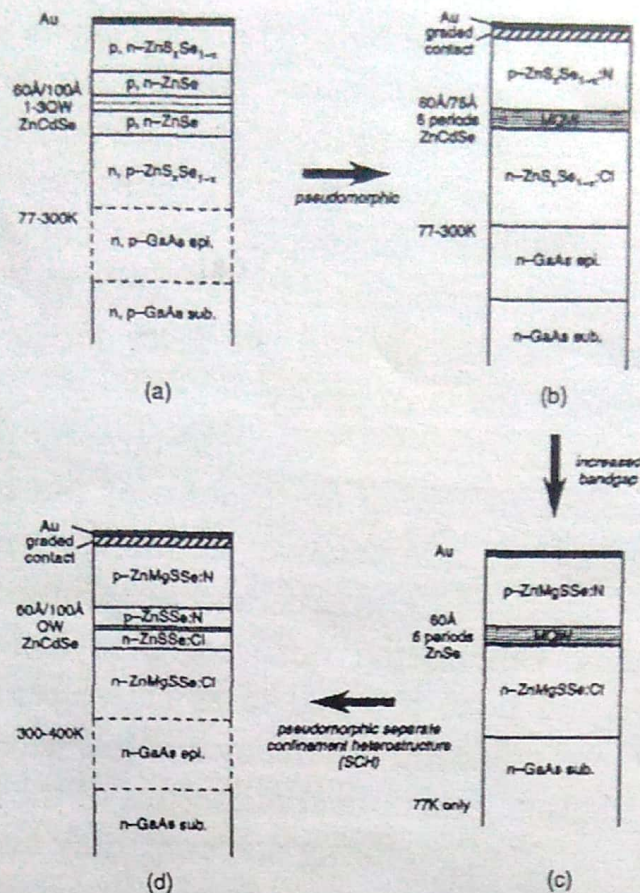


**Fig. 9.5.** Schematic diagrams of key blue/green laser diode configurations and their evolution from the initial laser design to the later laser design. [L.A. Kolodziejcki, R.L. Gunshor, and A.V. Nurmikko, *Ann. Rev. Mater. Sci.* **25**, 711 (1995).]

the operation of a bipolar transistor, by applying a small current to the base, a large amount of current can flow from the emitter to the collector if the gain is high. Comparing to the conventional bipolar junction transistor, the HBT offers an advantage of reduction of hole injection into the emitter, due to the valence band discontinuity. The barrier to the hole injection is exponentially sensitive to the valence band offset,  $\Delta E_v$ .

### 9.6.2. Quantum dot devices

The key parameter that controls the wavelength is the size of the dot. Large sized dots emit at longer wavelengths than small sized ones. Quantum dot heterostructures are commonly synthesized by molecular beam epitaxy at the initial stages of strained heteroepitaxial growth via the layer-island or Stranski-Krastanov growth mode.<sup>112,113</sup>

Quantum dots have been established their use in lasers and detectors. Quantum dot lasers with ultralow-threshold current densities and low sensitivity to temperature variations have been demonstrated.<sup>114,115</sup> Intersublevel detectors made of quantum dot nanostructures were found

not sensitive to normal-incidence light.<sup>116</sup> For the lasers using the quantum dot media often suffer from insufficient gain for the device to operate at the ground state wavelength, due to the combined consequence of the low density of states and the low area density of dots that is normally used. Several techniques have been developed to overcome this barrier. For example, several layers of quantum dots are used to increase the modal gain. Other methods include coating the laser facets to increase their reflectivity and lengthen the laser cavity.

The efficiency of luminescence from quantum dot structures depends on a number of factors including the capture of the carriers within the dots, the minimization of nonradiative recombination channels within the dots and in the surrounding matrix, and the elimination of defects at the hetero-interfaces. Embedding quantum dots inside an appropriate quantum well structure (also referred to as active region) demonstrated dramatically enhanced emission efficiency and low threshold current, due to the improved structural and optical properties of the embedding layers, and the enhanced ability of capturing and confining carriers to the vicinity of the dots.<sup>117,118</sup> Further structural improvement can be achieved by sandwiching quantum dots in a compositionally graded quantum well.<sup>119</sup> When the quantum dots of InAs are inserted at the center of compositionally graded  $\text{In}_x\text{Ga}_{1-x}\text{As}$  layers, the relative emission efficiency has been increased by nearly an order of magnitude over the emission of dots inside a constant composition (In,Ga)As structure.

## 9.7. Nanomechanics

In the previous two chapters, we have discussed the applications of SPM in the field of imaging surface topography and measurement of local properties of sample surface (Chapter 8) and nano manipulation and nanolithography in fabrication and processing of nanodevices. In this chapter, we will briefly introduce another important application of SPM, i.e. nanodevices derived from SPM. Although many devices are being investigated and more are to be developed in the conceivable future, we will take two examples to illustrate the possibilities and general approaches, specifically, nanosensors and nanotwizers.

Lang *et al.*<sup>120</sup> made an excellent summary of the applications of AFM cantilever based sensors in their tutorial article. When the surface of a cantilever or a tip is functionalized in such a way that a chemically active and a chemically inactive surface is obtained, chemical or physical processes on the active cantilever surface can be observed using the temporal

<http://hhud.tyu.edu.vn>

evolution of the cantilever's response. Cantilevers can be used as a nanomechanical sensor device for detecting chemical interactions between binding partners on the cantilever surface and in its environment. Such interactions might be produced by electrostatic or intermolecular forces. At the interface between an active cantilever surface and the surrounding medium, the formation of induced stress, the production of heat or a change in mass can be detected. In general, detection modes can be grouped into three strands: static mode, dynamic mode and heat mode as illustrated in Fig. 9.6.<sup>120</sup>

In the static mode, the static bending of the cantilever beam due to external influences and chemical/physical reactions on one of the cantilever's surfaces is investigated. The asymmetric coating with a reactive layer on one surface of the cantilever favors preferential adsorption of molecules on this surface. In most cases, the intermolecular forces in the adsorbed molecule layer produce a compressive stress, i.e. the cantilever bends. If the reactive coating is polymer and adsorbing molecules can diffuse, the reactive coating will swell and the cantilever beam will bend.

Similarly, if the cantilever beam emerges into a chemical or biochemical solution, the asymmetric interaction between the cantilever beam and the surrounding environment results in bending of the cantilever beam. Many new concepts and devices have been explored.<sup>121-124</sup>

In dynamic mode, the cantilever is driven at its resonance frequency. If the mass of the oscillating cantilever changes owing to additional mass

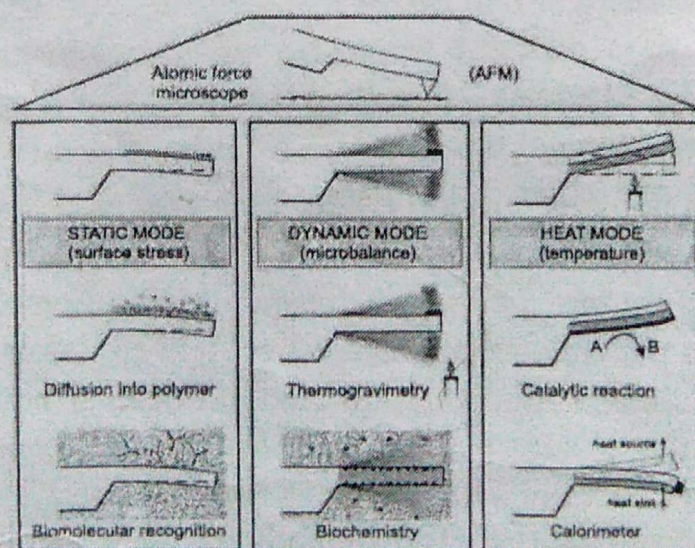


Fig. 9.6. AFM cantilever based sensors with detection modes being grouped into three strands: static mode, dynamic mode and heat mode. [H.P. Lang, M. Hegner, E. Meyer, and Ch. Gerber, *Nanotechnology* 13, R29 (2002).]

deposited on the cantilever, or if mass is removed from the cantilever, its resonance frequency changes. Using electronics designed to track the resonance frequency of the oscillating cantilever, the mass changes on the cantilever are derived from shifts of resonance frequency. The cantilever can be regarded as a tiny microbalance, capable of measuring mass changes of less than 1 pg.<sup>125</sup> In dynamic mode, active coatings should apply on both surfaces of the cantilever to increase the active surface where the mass change takes places. Dynamic mode works better in gas than in liquid, which complicates the exact determination of the resonance frequency of the cantilever. More examples are available in Ref. 126.

In heat mode, the cantilever is coated asymmetrically, one surface with a layer having a different thermal expansion coefficient than that of the cantilever itself. When such a cantilever is subjected to a temperature change, it will bend. Deflections corresponding to temperature changes in the micro-Kelvin range can be easily measured. If the coating is catalytically active, e.g. a platinum layer facilitates the reaction of hydrogen and oxygen to form water. In such a case, heat is generated on the active surface and will result in bending of the cantilever. Such a method can also be used in the study of phase transition and measurement of thermal properties of a very small amount of materials.<sup>127,128</sup>

Although the above discussion has been limited on the single cantilever nanosensors, the same principle is readily applicable to multiple cantilever nanosensors. For example, a SPM cantilever array consisting of more than 1000 cantilevers have been fabricated.<sup>129</sup>

## 9.8. Carbon Nanotube Emitters

There have been numerous reports describing studies on carbon nanotubes as field emitters,<sup>130-136</sup> since the discovery of carbon nanotubes. Standard electron emitters are based either on thermionic emission of electrons from heated filaments with low work functions or field emission from sharp tips. The latter generates monochromatic electron beams; however, ultrahigh vacuum and high voltages are required. Further, the emission current is typically limited to several microamperes. Carbon fibers, typically 7  $\mu\text{m}$  in diameter, have been used as electron emitters; however, they suffer from poor reproducibility and rapid deterioration of the tip.<sup>137</sup> Carbon nanotubes have high aspect ratios and small tip radius of curvature. In addition, their excellent chemical stability and mechanical strength are advantageous for application in field emitters. Rinzler *et al.*<sup>132</sup> demonstrated laser-irradiation-induced electron field emission from an individual multiwall

nanotube. Although the emission current of a single tube is constrained because of its very small dimensions, an array of nanotubes oriented perpendicular to an electrode would make an efficient field emitter.

De Heer and co-workers first demonstrated a high-intensity electron gun based on field emission from an array of oriented carbon nanotubes.<sup>130</sup> Field emission current densities of  $\sim 0.1 \text{ mA/cm}^2$  were observed when a voltage of 200 V was applied, and a current density of  $>100 \text{ mA/cm}^2$  was realized at 700 V. The gun was reported to be air stable and inexpensive to fabricate, and functions stably and reliably for long time. However, later research found a gradual degradation with time of the emission performances on both single-wall carbon nanotube and multi-wall carbon nanotube emitters.<sup>135</sup> The degradation was explained by the destruction of nanotubes by ion bombardment with ions either from gas phase ionization or anode emission. It was also found that the degradation of single-wall carbon nanotube emitter is significantly faster (a factor  $\geq 10$ ), since they are more sensitive to electron or ion bombardment.

A flat panel display based on nanotube field emission was also demonstrated.<sup>134</sup> A  $32 \times 32$  matrix-addressable diode nanotube display prototype was fabricated and a steady emission was produced in  $10^{-6}$  torr vacuum. Pixels were well defined and switchable under a half-voltage "off-pixel" scheme. A fully sealed field emission display of 4.5 inch in size has been fabricated using single-wall carbon nanotube—organic binders.<sup>138</sup> The nanotubes were vertically aligned using paste squeeze and surface rubbing techniques, and fabricated displays were fully scalable at temperatures as low as  $415^\circ\text{C}$ . The turn-on field of  $1 \text{ V}/\mu\text{m}$  and brightness of  $1800 \text{ cd/m}^2$  at  $3.7 \text{ V}/\mu\text{m}$  was observed on the entire 4.5 inch area from the green phosphor-indium-tin-oxide glass. Figure 9.7 shows a CRT lighting element equipped with aligned CNT emitters and the electron tube is 20 mm in diameter and 75 mm long.<sup>139</sup> A test of this cathode-ray tube lighting element suggested a lifetime of exceeding 10,000 h.<sup>139</sup>

Field emission properties of carbon nanotubes have been studied extensively. It was found that both aligned<sup>130,134,140</sup> and randomly<sup>133,135,141,142</sup> oriented nanotubes have impressive emission capabilities. Chen *et al.*<sup>143</sup> compared field emission data from aligned high-density carbon nanotubes with orientations parallel,  $45^\circ$ , and perpendicular to the substrate. The different orientations were obtained by changing the angle between the substrate and the bias electrical field direction. It was found that carbon nanotubes all demonstrated efficient field emission regardless of their orientations. The nanotube arrays oriented parallel to the substrate have a lower onset applied field, and a higher emission current density under the same electric field than those

<http://hhud.tyu.edu.vn>

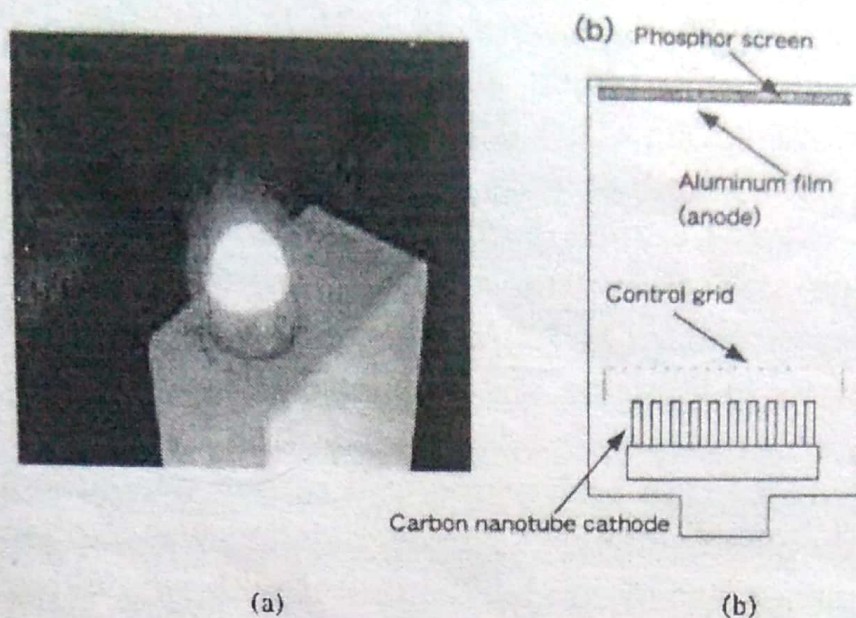


**Fig. 9.7.** A CRT lighting element equipped with aligned CNT emitters on SUS304 (a) operating device and (b) structure. The electron tube is 20 mm in diameter and 75 mm long. [H. Murakami, M. Hirakawa, C. Tanaka, and H. Yamakawa, *Appl. Phys. Lett.* **76**, 1776 (2000).]

oriented perpendicular to the substrate. The result indicates that electrons can emit from the body of nanotubes and carbon nanotubes can be used as linear emitter. The ability to emit electrons from the body of nanotubes was attributed to the small radius of the tubes and the presence of defects on the surface of carbon nanotubes. Saito and co-workers<sup>144,145</sup> have conducted field emission microscopy of single-wall nanotubes and open multiwall nanotubes. In addition to field emitters, carbon nanotubes have been explored for many other applications including sensors, scanning probe tips, hydrogen storage and Li batteries as summarized in an excellent review paper by Terrones.<sup>146</sup>

## 9.9. Photoelectrochemical Cells

The development of photoelectrochemical cells, also commonly known as photovoltaic cells or solar cells, emphasizes the need for a higher conversion efficiency of solar energy to electrical power. Photoelectrochemical devices consisting of silicon-based p-n junction materials<sup>147,148</sup> and other heterojunction materials,<sup>148-150</sup> most notably indium-gallium-phosphide/gallium-arsenide and cadmium-telluride/cadmium-sulfide, have been extensively studied for efficient light conversion, and have obtained the highest efficiency close to 20%<sup>147,148</sup> as compared to cells based on other



materials. However, the high cost of production, expensive equipment, and necessary clean-room facilities associated with the development of these devices have directed exploration of solar energy conversion to cheaper materials and devices.

Sol-gel-derived titania films with a crystal structure of anatase and a mesoporous structure have been demonstrated as an excellent material for photoelectrochemical cells and have gained a lot of attention since its introduction by O'Regan and Grätzel.<sup>151</sup> Such devices are commonly referred to as dye-sensitized solar cells consisting of porous nanocrystalline titania ( $\text{TiO}_2$ ) film in conjunction with an efficient light-absorbing dye, and have shown an impressive energy conversion efficiency of  $>10\%$  at lower production costs.<sup>152-155</sup> Figure 9.8 shows the operation schematic of such a dye-sensitized mesoporous titania photovoltaic cell and a SEM micrograph of a mesoporous anatase titania film.<sup>155</sup> In such devices,  $\text{TiO}_2$  functions as a suitable electron-capturing and electron-transporting material with a conduction band at 4.2 eV and an energy band gap of 3.2 eV, corresponding to an absorption wavelength of 387 nm.<sup>156</sup> In this process, the dye adsorbed to  $\text{TiO}_2$  is exposed to a light source, absorbs photons upon exposure, and injects electrons into the conduction band of the  $\text{TiO}_2$  electrode. Regeneration of the dye is initiated by subsequent hole-transfer to the electrolyte and electron capture after the completion of the  $\text{I}^-/\text{I}_3^-$  redox couple at the solid electrode-liquid electrolyte interface.

Nanostructures are advantageous for photoelectrochemical cell devices for high efficient conversion of light to electrical power due to its large

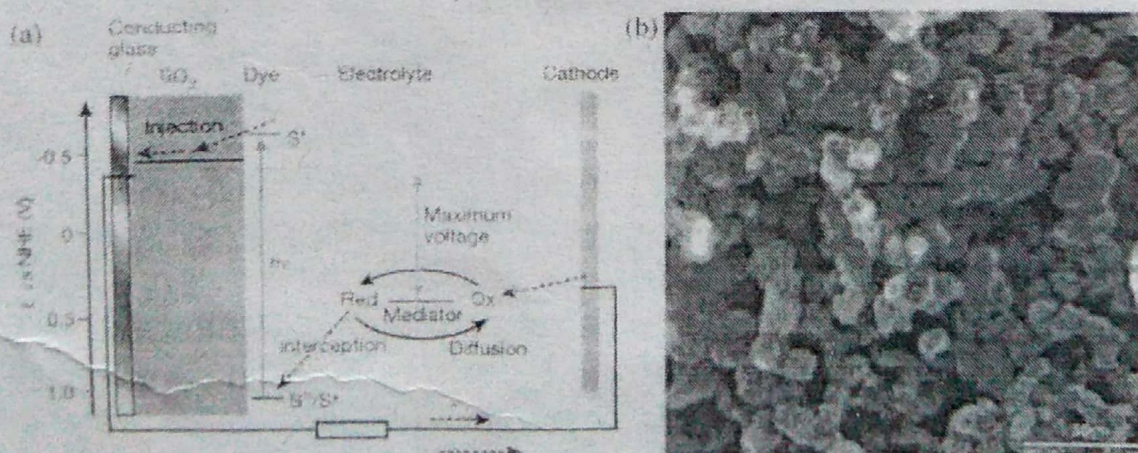


**Fig. 9.8.** (a) The operation schematic of such a dye-sensitized mesoporous titania photovoltaic cell and (b) a SEM micrograph of a mesoporous anatase titania film. [M. Grätzel, *Nature* **414**, 338 (2001).] <http://hhud.tvu.edu.vn>

surface area at which photoelectrochemical processes take place. Many techniques have been investigated to synthesize  $\text{TiO}_2$  electrodes to improve the structure for more efficient electron transport and good stability. Chemical vapor deposition of  $\text{Ti}_3\text{O}_5$  has been utilized to deposit layered crystalline anatase  $\text{TiO}_2$  thin films that are optically responsive and stable.<sup>156</sup> Gas-phase hydrothermal crystallization of  $\text{TiCl}_4$  in aqueous mixed paste has been done to obtain crack-free porous nanocrystalline  $\text{TiO}_2$  thick film through low-temperature processing.<sup>157</sup> Compression techniques of  $\text{TiO}_2$  powder have also been used to form porous and stable films.<sup>158</sup> The most common and widely used technique for the preparation of crack-free  $\text{TiO}_2$  thick film for use as suitable electron-transporting electrodes involves the preparation of  $\text{TiO}_2$  paste by way of sol-gel processing of commercially-available  $\text{TiO}_2$  colloidal precursors containing an amount of organic additives and followed with hydrothermal treatment. This conventional method requires the deposition of the prepared paste by either doctor-blading, or spin coating, or screen-printing on a transparent conducting substrate.<sup>159-161</sup> Moderate temperature sintering is utilized to remove the organic species and to connect the colloidal particles. Typical thickness of mesoporous  $\text{TiO}_2$  film<sup>153-155</sup> using this method ranges from 2  $\mu\text{m}$  to 20  $\mu\text{m}$ , depending on the colloidal particle size and the processing conditions, and the maximum porosity obtained by this technique has reported to be  $\sim 50\%$  with an average pore size around 15 nm and internal surface area of  $> 100 \text{ m}^2/\text{g}$ .

Although various techniques have been utilized and explored to synthesize a more efficient structure of  $\text{TiO}_2$  film to enhance the electrical and photovoltaic properties of solar cell devices, the capability of these devices to surpass the 10% light conversion efficiency has been hindered. Efforts to find other solar cell devices with various broad-band semiconducting oxide materials, including  $\text{ZnO}$ <sup>162-164</sup> and  $\text{SnO}_2$ <sup>164,165</sup> films, have been made for possible improvement of the current state of  $\text{TiO}_2$ -based dye-sensitized solar cell devices. Composite structures consisting of a combination of  $\text{TiO}_2$  and  $\text{SnO}_2$ ,  $\text{ZnO}$  or  $\text{Nb}_2\text{O}_5$  materials,<sup>164,166,167</sup> or a combination of other oxides,<sup>168-170</sup> have also been examined in an attempt to enhance the overall light conversion efficiency. In addition, hybrid structures comprised of a blend of semiconducting oxide film and polymeric layers for solid-state solar cell devices have been explored in an effort to eliminate the liquid electrolyte completely for increased electron transfer and electron regeneration in hopes of increasing the overall efficiency.<sup>171-173</sup> So far, these devices have achieved an overall light conversion efficiency of up to 5% for  $\text{ZnO}$  devices,<sup>162</sup> up to 1% for  $\text{SnO}_2$  devices,<sup>165</sup> up to 6% for composite devices,<sup>165</sup> and up to 2% for hybrid devices,<sup>171</sup> all of which are still less efficient than solar cell devices based on dye-sensitized  $\text{TiO}_2$  mesoporous film.

## 9.10. Photonic Crystals and Plasmon Waveguides

### 9.10.1. Photonic crystals

Photonic crystals have a broad range of applications.<sup>174,175</sup> Examples readily for commercialization include waveguides and high-resolution spectral filters. Photonic crystals allow for guiding geometries such as 90° corners.<sup>176</sup> Potential applications are photonic crystal lasers, light emitting diodes and photonic crystal thin films to serve as anticounterfeit protection on credit cards. Ultimately, it is hoped that photonic crystal diodes and transistors will eventually enable the construction of an all-optical computer.

A photonic-band-gap (PBG) crystal, or simply referred to as photonic crystal, is a spatially periodic lattice consisting of alternating regions of dielectric materials with different refractive indices.<sup>177</sup> The concept of PBG crystals was first proposed by Yablonovitch<sup>178</sup> and John<sup>179</sup> in 1987, and the first experimental realization of 3D photonic crystal was reported in 1991.<sup>180</sup> Figure 9.9 shows a schematic of one-, two-, and three-dimensional photonic crystals. Because of its long-range order, a photonic crystal is capable of controlling the propagation of photons in much the same way as a semiconductor does for electrons: that is, there exists a forbidden gap in the photonic band structure that can exclude the existence of optical modes within a specific range of frequencies. A photonic band gap provides a powerful means to manipulate and control photons, and can find many applications in photonic structures or systems. For example, photonic crystals can be used to block the propagation of photons irrespective of their polarization direction, localize photons to a specific area at restricted frequencies, manipulate the dynamics of a spontaneous or stimulated emission process, and serve as a lossless waveguide to confine or

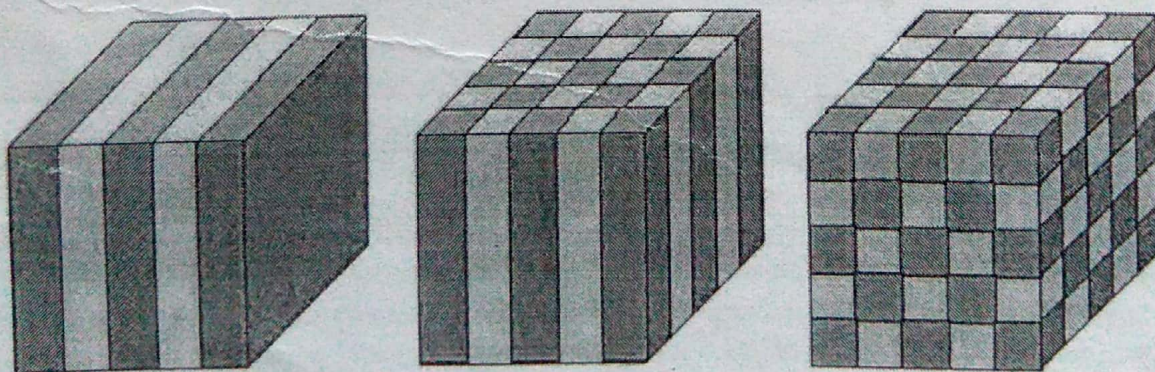
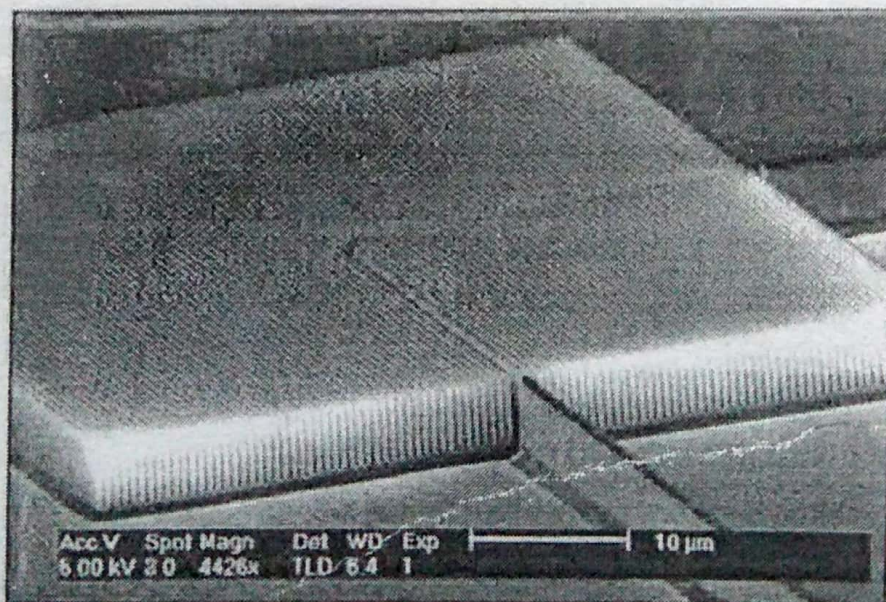


Fig. 9.9. Schematic representing one-, two-, and three-dimensional photonic crystals consisting of alternating regions of dielectric materials.

direct the propagation of light along a specific channel). It should also be noted that photonic crystals work at all wavelengths and, thus, find applications in the near-infrared telecommunication window or visible region if the size of the periodic structures (lattice constants) is appropriately chosen. A number of methods have been explored for the fabrication of photonic crystals.<sup>181</sup> Examples include layer-by-layer stacking techniques<sup>182,183</sup> electrochemical etching,<sup>184</sup> chemical vapor deposition,<sup>185</sup> holographic lithography,<sup>186</sup> and self-assembly of monodispersed spherical colloids.<sup>187,188</sup> Figure 9.10 shows SEM micrograph of a periodic array of silicon pillars fabricated using deep anisotropic etching. The silicon pillars are 205 nm in diameter and 5  $\mu\text{m}$  tall. This structure possesses a band gap of  $\sim 1.5 \mu\text{m}$  for transverse magnetic polarization. By removing an array of pillars, a waveguide bend is fabricated. Input and output waveguides are integrated with the two-dimensional photonic crystal.<sup>189</sup>

A complete or full band gap is defined as the one that can extend over the entire Brillouin zone in the photonic band structure.<sup>190</sup> An incomplete band gap is often referred to as a pseudo gap, because it appears only in the transmission spectrum along a certain direction of propagation. A complete band gap can be considered as a set of pseudo gaps that overlap for a certain range of frequencies over all three dimensions of space.



**Fig. 9.10.** SEM micrograph of a periodic array of silicon pillars fabricated using deep anisotropic etching. The silicon pillars are 205 nm in diameter and 5  $\mu\text{m}$  tall. This structure possesses a band gap of  $\sim 1.5 \mu\text{m}$  for transverse magnetic polarization. By removing an array of pillars, a waveguide bend is fabricated. Input and output waveguides are integrated with the photonic crystal. [T. Zijlstra, E. van der Drift, M. J. A. de Dood, E. Snoeks, and A. Polman, *J. Vac. Sci. Technol.* **B17**, 2734 (1999).]

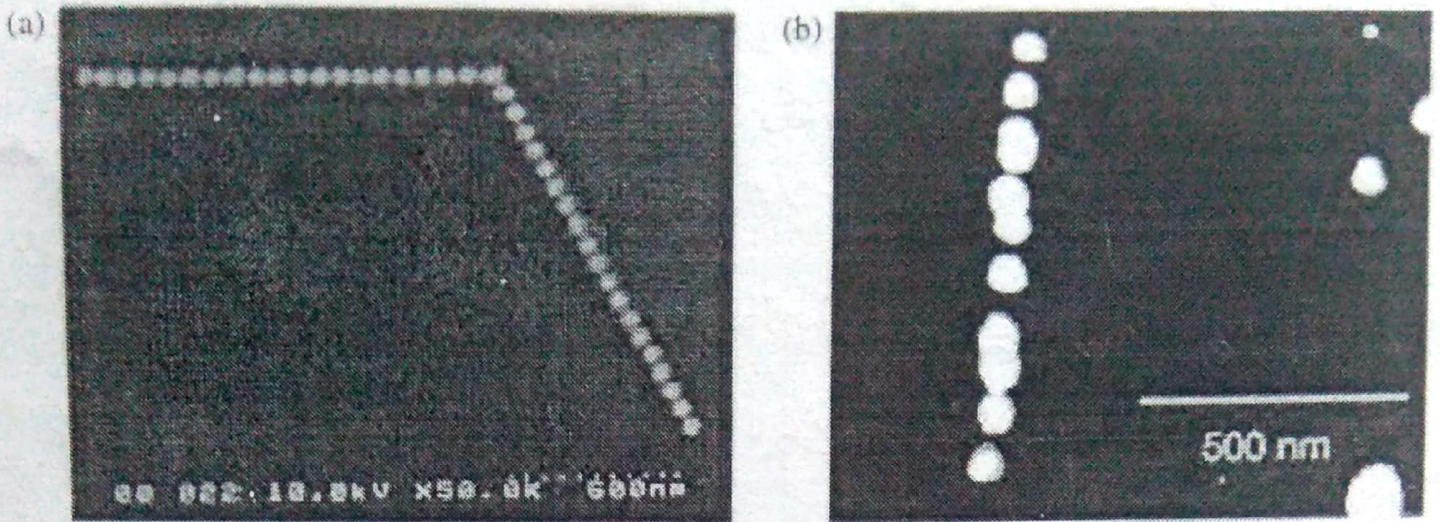


**Fig. 9.11.** (a) SEM image of a  $60^\circ$  corner in a plasmon waveguide, fabricated using electron beam lithography. The gold dots are  $\sim 50$  nm in diameter and spaced by  $\sim 75$  nm (center-to-center). (b) Straight plasmon waveguide made using 30 nm diameter colloidal gold nanoparticles. The particles were assembled on a straight line using an AFM in contact mode, and subsequently imaged in non-contact mode. [S.A. Maier, M.L. Brongersma, P.G. Kik, S. Meltzer, A.A.G. Requicha, and H.A. Atwater, *Adv. Mater.* **13**, 1501 (2001).]

### 9.10.2. Plasmon waveguides

Plasmon waveguides are optical devices based on surface plasmon resonance of noble metal nanoparticles. The surface plasmon resonance is due to the strong interaction between the electric field of light and free electrons in the metal particle, which has been discussed in the previous chapter. Arrays of closely spaced metal nanoparticles set up coupled plasmon modes that give rise to coherent propagation of electromagnetic energy along the array via near-field coupling between adjacent particles.<sup>191-193</sup> The dipole field resulting from a plasmon oscillation in a single metal nanoparticle can induce a plasmon oscillation in a closely spaced neighboring particle due to near field electrodynamic interactions.<sup>193,194</sup> It has been shown that electromagnetic wave can be guided on a scale below the diffraction limit and around  $90^\circ$  corners or bending radius  $\ll$  wavelength of light as shown in Fig. 9.11.<sup>191</sup> Electron beam lithography and AFM nanomanipulation have been applied to fabricate plasmon waveguides with gold nanoparticles of 30 and 50 nm in diameter, and the center-to-center space was three times of the particle radius.<sup>191</sup>